

# Hexokinase 1 blocks apoptotic signals at the mitochondria

Anja Schindler, Edan Foley\*

Department of Medical Microbiology and Immunology, University of Alberta, Edmonton, AB T6G 2S2, Canada



## ARTICLE INFO

### Article history:

Received 13 August 2013

Accepted 30 August 2013

Available online 7 September 2013

### Keywords:

TNF

Apoptosis

Hexokinase

Mitochondria

Mitochondrial membrane potential

Bcl-2 proteins

## ABSTRACT

To coordinate a meaningful response to infection or tissue damage, Tumor Necrosis Factor (TNF) triggers a spectrum of reactions in target cells that includes cell activation, differentiation, proliferation and death. Deregulated TNF signaling can lead to tissue damage and organ dysfunction during inflammation. Previously, we identified hexokinase 1 (HK1) as a potent pro-survival factor that counters TNF-induced apoptosis in type II cells. Here we used HK1 siRNA and clotrimazole to generate mitochondrial depletion phenotypes of HK1 to test if HK1 acts at the mitochondria to block TNF-induced apoptosis. We found that HK1 is predominantly mitochondrial in type II cells and that its depletion at the mitochondria decreased the inner mitochondrial membrane potential and accelerated TNF-induced apoptosis. In addition, we showed that the decrease of the mitochondrial membrane potential after HK1 depletion depended on the presence of Bak and Bax and was blocked by Bcl-2 overexpression. From these findings, we conclude that HK1 counters TNF-induced apoptosis through antagonization of pro-apoptotic Bcl-2 proteins at the outer mitochondrial membrane.

© 2013 Elsevier Inc. All rights reserved.

## 1. Introduction

Inflammation is an innate immune reaction that aims at the resolution of tissue infection or tissue damage [1]. Tissue resident macrophages, dendritic cells and mast cells induce inflammation through the secretion of second messengers such as the prototypic tumor necrosis factor alpha (TNF- $\alpha$ , mostly abbreviated as TNF) cytokine [1,2]. TNF signals through a nuclear factor-kappa B (NF- $\kappa$ B), a mitogen-activated protein kinase (MAPK), and a caspase module in target cells [3]. The TNF receptor complex at the cell membrane (complex I) activates the NF- $\kappa$ B and MAPK modules to promote inflammation and survival [4]. Recruitment of caspase-8 during receptor endocytosis converts the immunogenic complex I into the pro-apoptotic complex II [4,5]. However, under default conditions, NF- $\kappa$ B dependent anti-apoptotic gene products prevent the activation of caspase-8 in complex II [4,6].

Restricted NF- $\kappa$ B activity permits the activation of the pro-apoptotic caspase cascade [4]. In type I cells, such as lymphocytes, caspase-8 directly activates downstream effector caspases such as caspase-3 and -7 [7–9]. Caspase-8 does not directly induce apoptosis in type II cells, such as liver, pancreatic  $\beta$ -cells, or HeLa cells. These cells depend on the caspase-8 induced release of pro-apoptotic factors from the mitochondria to activate effector caspases [7–9]. Specifically, caspase-8 processes the BH3-only protein Bid to generate truncated Bid (tBid)

[3,10]. tBid activates the Bcl-2 effector proteins Bak and Bax [10–12]. Bax resides in the cytoplasm or associates with the periphery of the outer mitochondrial membrane (OMM) [11]. Bak is stabilized at the OMM stabilized by voltage dependent anion channel 2 (VDAC2) and anti-apoptotic Bcl-2 proteins [11]. tBid-induced conformational changes trigger Bax translocalization to the mitochondria and oligomerization and insertion of both Bax and Bak into the OMM [10,12]. Bax and Bak oligomers form toroidal pores in the OMM that release pro-apoptotic factors, such as cytochrome c, from the intermembrane space (IMS) of mitochondria [10,13]. As apoptosis progresses, the mitochondrial permeability transition pore (MPTP) allows unselective ion flux across the inner mitochondrial membrane (IMM) [13]. The IMM potential dissipates and the mitochondrial matrix swells, leading to rupture of the OMM and the release of more pro-apoptotic molecules from the IMS [10,13]. Cytochrome c activates caspase-9 in the apoptosome complex, which in turn activates effector caspases to initiate all biochemical and morphological changes associated with apoptosis [14–17]. Effector caspases also contribute to a pro-apoptotic feedback loop that proceeds through enhanced caspase-8 activation [17].

We previously identified hexokinase 1 (HK1) as an anti-apoptotic protein in type II cells [18]. The ubiquitous HK1 predominantly channels phosphorylated glucose into catabolic pathways to generate ATP [19]. Like HK2, HK1 interacts with the OMM in a dynamic manner that is mediated by 15 hydrophobic N-terminal amino acids [20–22]. Growth factors promote the interaction of HKs with the mitochondria, and the interaction of HK2 with the mitochondria prevents intrinsic apoptosis [23–25]. Several overexpression studies implicated similar roles for HK1 in the inhibition of intrinsic apoptosis [23,26,27]. We found that targeted depletion of HK1 with siRNA sensitized a variety

**Abbreviations:** TNF, tumor necrosis factor alpha; NF- $\kappa$ B, nuclear factor-kappa B; VDAC, voltage dependent anion channel; IMS, intermembrane space; MPTP, mitochondrial permeability transition pore; IMM, inner mitochondrial membrane; HK, hexokinase; siRNA, small interfering RNA.

\* Corresponding author at: University of Alberta, Medical Microbiology and Immunology, 6-71 HMRC, Edmonton, AB T6G 2S2, Canada. Tel.: +1 780 492 2303.

E-mail address: [efoley@ualberta.ca](mailto:efoley@ualberta.ca) (E. Foley).

of type II cells to the induction of apoptosis by extrinsic TNF cues [18]. However, our studies did not establish the mechanism by which HK1 blocks apoptotic cues.

In this report, we show that the majority of HK1 in type II cell lines localized to the mitochondria, and that depletion of HK1 or detachment of mitochondrial HKs decreased the IMM potential and accelerated TNF-induced apoptosis. Cells that were deficient in Bak and Bax or overexpressed the Bak and Bax antagonist Bcl-2 resisted to the decrease of the IMM potential after HK1 depletion. Furthermore, we found that loss of HK1 constitutively increased the amounts of mitochondrial Bax, and accelerated Bax oligomerization and release of mitochondrial cytochrome c in the presence of TNF. These findings suggest that mitochondrial HK1 antagonizes pro-apoptotic Bcl-2 proteins to stabilize mitochondrial integrity and attenuate TNF-induced apoptosis.

## 2. Materials and methods

### 2.1. Cell culture

All cells were cultured at 37 °C and 5% CO<sub>2</sub> in Dulbecco's Modified Eagle Medium with 4.5 g/l D-glucose and L-glutamine and sodium bicarbonate (Sigma, D5796) supplemented with 10% (v/v) fetal bovine serum (GIBCO), 50 U/ml penicillin and 50 µg/ml streptomycin (GIBCO). In addition, MEF and Bak<sup>-/-</sup>, Bax<sup>-/-</sup> DKO MEF cells were supplemented with 2 mM L-glutamine (GIBCO) and 1% (v/v) MEM non-essential amino acids (GIBCO).

### 2.2. Cell treatments

HeLa cells were treated with 20 ng/ml TNF-α (Roche) to induce survival signaling or 20 ng/ml TNF-α and 5 µg/ml cycloheximide (Sigma) to induce apoptosis. The general caspase inhibitor z-VAD-fmk (R&D Systems) in DMSO was added at a concentration of 25 µM on day 2 following transfection with HK1 siRNA. Unless indicated otherwise, 20 µM clotrimazole (CTZ, Sigma) in DMSO were added in serum-free culture medium to cells that were previously washed twice with serum-free culture medium. When CTZ treatment was combined with an apoptotic stimulus of TNF and cycloheximide, CTZ treatment in serum-free medium was administered from 2 to 4 h after TNF and cycloheximide treatment.

### 2.3. siRNA transfections

HeLa cells were transfected with HK1 siRNA (Applied Biosystems) or a non-silencing control siRNA (Qiagen, AllStars Negative Control). MEF cells were transfected with a mouse HK1 siRNA (Applied Biosystems) or a non-silencing control siRNA (Applied Biosystems, Silencer Select negative control #1 siRNA).

For transfections in 12-well format, 100 µl of a 200 nM siRNA predilution in sterile nuclease-free water (HyClone) and 150 µl transfection mixture containing 2 µl DharmaFECT 1 Transfection Reagent (Dharmacon) and 148 µl OptiMEM (GIBCO) were prepared in microfuge tubes and incubated for 5 min at room temperature. siRNA predilution and transfection mixture were mixed and incubated for 30 min at room temperature, and then transferred into 12-well plates.  $1 \times 10^5$  HeLa or  $7.5 \times 10^4$  MEF cells in 750 µl antibiotic-free culture medium were added to the siRNA transfection mixture. Cells were incubated for 72 h. For siRNA transfections that were followed by DNA transfections 2 days later,  $1.125 \times 10^5$  HeLa cells were seeded into 12-well plates. For siRNA transfections in 6-well format, all volumes were scaled up by the factor 2, and  $2.25 \times 10^5$  HeLa cells were seeded.

### 2.4. DNA expression constructs

HK1 cDNA (variant 1) was purchased from Open Biosystems. To generate a carboxyl-terminally tagged full-length HK1-GFP, HK1 cDNA was amplified with a forward primer that contained a SacI restriction site (5'-AATTGAGCTCATGATCGCCGCGCAGCTCTG-3') and a reverse primer that contained a PstI restriction site and eliminated the carboxyl-terminal stop codon (5'-AATTCTGCAGGCTGCTGCCTCTGTGCGTAAAC-3'). The PCR product were subcloned into the vector pEGFP-N1. All constructs were verified for their respective sequence.

### 2.5. DNA transfections

For the transfection of HK1 expression constructs or the empty vector control,  $4.5 \times 10^5$  HeLa cells were plated into each well of a 6-well plate 1 day prior to transfection. On the following day, each well was washed once with PBS, and the medium was replaced with 500 µl OptiMEM (GIBCO). A DNA predilution of 2 µg DNA in 250 µl OptiMEM and 250 µl transfection mixture containing 4 µl Lipofectamine 2000 (Invitrogen) and 246 µl OptiMEM were prepared in microfuge tubes and incubated for 5 min at room temperature. The DNA predilution and transfection mixture were mixed, incubated for 20 min at room temperature, and then added dropwise to each well. After 5 h, cells were recovered by the addition of 1 ml antibiotic-free culture medium containing 20% (v/v) fetal bovine serum.

For the transfection of the Bcl-2 expression construct or the empty vector control into HeLa cells that had been transfected with siRNA for 2 days in 12-well plates, a DNA pre-dilution of 2 µg DNA in 125 µl OptiMEM and transfection mixture of 3 µl DharmaFECT Duo Transfection Reagent (Dharmacon) in 122 µl OptiMEM were prepared and added to 250 µl OptiMEM in the well. Cell recovery was carried out with 500 µl antibiotic-free culture medium containing 20% fetal bovine serum.

### 2.6. Confocal fluorescence microscopy

$3.5 \times 10^5$  HeLa cells were plated onto coverslips (Electron Microscopy Sciences, 72224-01) in the wells of a 12-well plate. The following day, the cells were treated with 5 to 40 µM HK1 peptide or control peptide in serum-free culture medium for 1 h after 2 washes in serum-free culture medium, if applicable. The culture medium was aspirated and replaced with culture medium that contained 2 nM MitoTracker Red (Molecular Probes) and incubated for 30 min, if applicable. The cells were washed twice in PBS and fixed with 2% (v/v) formaldehyde (Sigma) in PBS for 15 min at room temperature. The cells were washed 3 times in PBS for 5 min each, permeabilized and blocked with 500 µl saponin buffer (0.2% (w/v) saponin, 0.1% (w/v) BSA, in PBS) 3 times for 5 min each, and incubated with a 1:100 dilution of anti-HK1 antibody (Cell Signaling, rabbit monoclonal, clone C35C4, #2024) in saponin buffer for 1 h at room temperature. The cells were then washed twice in saponin buffer for 5 min each and incubated with a 1:1000 dilution of goat anti-rabbit secondary antibody (Molecular Probes, goat polyclonal conjugated to Alexa Fluor 488) and a 1:1000 dilution of the nucleic acid stain Hoechst 33258 (Molecular Probes) in saponin buffer. The stained cells were fixed with 2% (v/v) formaldehyde in PBS for 15 min at room temperature, washed twice in PBS for 5 min each and mounted with Fluoromount (Sigma).

The images were acquired at 60X magnification with a spinning disk confocal fluorescence microscope (Olympus IX-81 with a CSU-X1 spinning disk confocal scan head (Yokogawa Electric Corporation)) integrated by Quorum WaveFX imaging software (Quorum Technologies) in the Faculty of Medicine and Dentistry Core Imaging Facility at the University of Alberta. The images were analyzed with Imaris software (Bitplane).

## 2.7. Cellular fractionation

An entire 6-well plate was set up for each experimental condition.  $9 \times 10^5$  HeLa or  $7 \times 10^5$  MEF cells were plated into each well, if the cellular fractionation was planned for the subsequent day;  $4.5 \times 10^5$  or  $2.25 \times 10^5$  HeLa cells were plated, if the cellular fractionation was planned to follow DNA or siRNA transfection, respectively. Where applicable, HeLa cells were treated with CTZ, HK1 amino-terminal peptide, or TNF and cycloheximide immediately prior to fractionation. Cells were harvested by trypsinization, and the cell pellet was washed twice in PBS and resuspended in 1 ml hypotonic fractionation buffer (200 mM mannitol; 70 mM sucrose; 10 mM HEPES, pH = 7.5; 1 mM EGTA, pH = 8.0), and incubated on ice for 10 min. The cell suspension was transferred to a pre-cooled 5 ml glass Potter–Elvehjem type tissue grinder with teflon pestle (Wheaton) connected to a drill press and lysed mechanically. The lysate was transferred into a pre-cooled microfuge tube, and unbroken cells and nuclei were precipitated through 2.5 min spins in a bench top centrifuge at  $700 \times g$  and  $4^\circ\text{C}$ . The heavy membrane fraction containing the mitochondria was precipitated from the remaining supernatant with a 15 min spin at  $7000 \times g$  and  $4^\circ\text{C}$  and washed twice with 500  $\mu\text{l}$  fractionation buffer and resuspended in 50  $\mu\text{l}$  fractionation buffer. The supernatant was spun for 30 min at maximum speed and  $4^\circ\text{C}$  to precipitate the majority of the light membrane fraction and to obtain the nearly pure cytosolic fraction. The protein content of all samples and fractions was adjusted, and 6X sample buffer (187.5 mM Tris, pH = 6.8; 30% (v/v) glycerol, 6% (w/v) SDS, 150 mM  $\beta$ -mercaptoethanol, 0.00375% (w/v) bromophenol blue) was added. The samples were boiled for 5 min and probed for the proteins of interest by Western blot analysis. VDAC1 served as a control for the heavy membrane/mitochondrial fraction and tubulin as a control for the cytosolic fraction.

## 2.8. Western blotting

In general, Western blot samples were prepared from the lysates of a near confluent cell population in one well of a 12-well plate or from cellular fractionations set up in 6-well plates. To this end, HeLa and MEF cells were plated as required by siRNA and/or DNA transfections. If applicable, cell treatments with CTZ and/or TNF and cycloheximide, or HK1 amino-terminal peptide were administered, and cellular fractionation and cross-linking were performed as described. Cells in 12-well plates that did not undergo cellular fractionation, were washed once in PBS, harvested by trypsinization and resuspended in 50  $\mu\text{l}$  lysis buffer (20 mM Tris, pH 7.5; 25 mM glycerol-3-phosphate; 150 mM NaCl; 1% Triton X-100; 2 mM  $\text{Na}_3\text{VO}_4$ ; protease inhibitors) or scraped into 50  $\mu\text{l}$  of lysis buffer. The soluble fraction of the lysates was added to 80  $\mu\text{l}$  2X sample buffer (62.5 mM Tris, pH 6.8; 10% (v/v) glycerol; 2% (w/v) SDS; 50 mM  $\beta$ -mercaptoethanol; 0.00125% (w/v) bromophenol blue; 8 M urea only for PARP1 blots) and boiled for 5 min. Proteins were separated by SDS-PAGE electrophoresis and transferred to a nitrocellulose membrane by semi-dry transfer. Membranes were blocked in blocking buffer (LI-COR Biosciences) for 1 h at room temperature and probed with primary antibodies against HK1 (Cell Signaling, rabbit monoclonal, clone C35C4), HK2 (Cell Signaling, rabbit monoclonal, clone C64G5), Bax (Trevigen, mouse monoclonal, clone YTH-2D2), cytochrome c (Millipore, mouse monoclonal, MAB1800), VDAC1 (Santa Cruz, mouse monoclonal, clone 20B12), tubulin (DSHB, mouse polyclonal, E7), PARP1 (Trevigen, mouse monoclonal, clone C2-10), caspase-9 (Cell Signaling, rabbit polyclonal, #9502) at a dilution of 1:1000 (or 1:2000 for the PARP1 antibody) in blocking buffer with 0.1% (v/v) Tween-20 for at least 3 h at room temperature or overnight at  $4^\circ\text{C}$ . The membranes were washed 4 times in PBS with 0.1% (v/v) Tween-20 for 5 min each at room temperature and incubated with a 1:10,000 dilution of the Alexa Fluor 680 or 750 conjugated goat anti-mouse or goat-anti rabbit IgG secondary antibodies (Molecular Probes)

in PBS with 0.1% (v/v) Tween-20 for 30 min at room temperature. The membranes were washed 4 times in PBS with 0.1% (v/v) Tween-20 for 5 min each, rinsed once in PBS, and visualized with the Aeries automated imaging system (LI-COR Biosciences) and Aeries 1.0 software (LI-COR Biosciences).

## 2.9. Measurement of the IMM potential in a cytometric assay with TMRE

In general, TMRE staining was conducted on a near confluent cell population from one well of a 12-well plate. To this end,  $4 \times 10^5$  HeLa were plated into each well of a 12-well plate, if the TMRE assay was planned for the subsequent day. HeLa and MEF cells that required siRNA and DNA transfections prior to staining were plated as indicated in the transfection protocols. If applicable, cells were treated with CTZ. In the last hour of the experiment, the cells were incubated with 1  $\mu\text{M}$  tetramethylrhodamine ethyl ester (TMRE, Molecular Probes) for 30 min at  $37^\circ\text{C}$  and then harvested by trypsinization. The cell pellet was washed in PBS and resuspended in 500  $\mu\text{l}$  PBS. The percentage of cells with a lower than healthy range of TMRE fluorescence per cell, was determined by flow cytometry (FACScan, Becton Dickinson) in the Faculty of Medicine and Dentistry Flow Cytometry Facility at the University of Alberta. The level of TMRE fluorescence was detected through the FL-2 channel equipped with a 585 nm filter (42 nm band pass). Data were acquired on 10,000 cells with fluorescence at logarithmic gain and analyzed with the CellQuest software (BD Biosciences).

## 2.10. Bax oligomerization

An entire 6-well plate with  $2.25 \times 10^5$  HeLa cells per well was transfected with siRNAs as described. On day 3, the cells were treated with TNF and cycloheximide, harvested by trypsinization, and lysed mechanically. The heavy membrane/mitochondrial fraction was isolated as described, washed once, and lysed in 500  $\mu\text{l}$  lysis buffer 2 (150 mM NaCl; 50 mM Tris, pH = 7.5; 5 mM EGTA, pH = 8.0; 2%

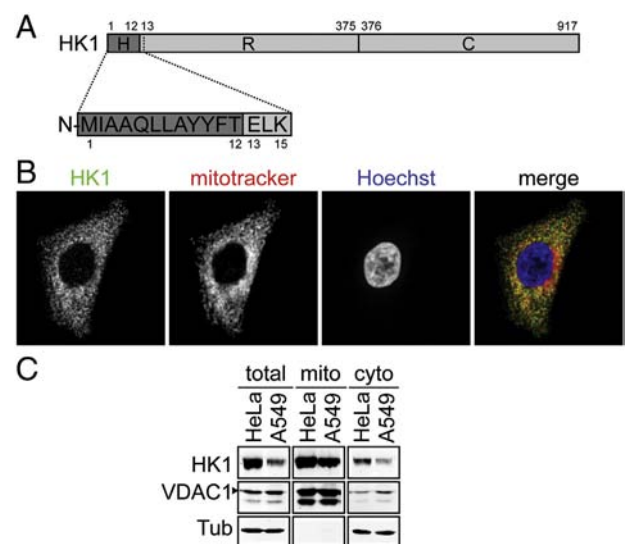


**Fig. 1.** HK1 is a mitochondrial protein. A: Illustration of the domain structure of HK1, including the hydrophobic N-terminus (H), the regulatory domain (R), and the C-terminal catalytic domain (C). The N-terminal 15 amino acids responsible for mitochondrial association of HK1 are shown. B: Confocal fluorescence microscopic image of HeLa cells that were stained with an antibody against endogenous HK1, MitoTracker Red, and nucleic acid stain Hoechst 33258. All single channel images were false-coloured (HK1 in green, MitoTracker Red in red, Hoechst in blue) and merged. C: Western blot of total, heavy membrane/mitochondrial (mito) and cytosolic (cyto) fractions from HeLa and A549 cells probed for HK1, VDAC1 and Tubulin (Tub). Tubulin and VDAC1 served as markers for cytosolic and mitochondrial fractions, respectively.



(w/v) CHAPS). The samples were incubated for 30 min on ice and spun in a bench top centrifuge for 10 min at maximal speed and 4 °C. The protein concentration of the supernatants was equalized. Each of the supernatants was split in half, and one of the samples was treated with 1 mM of the cross-linker bismaleimidoethane (BMH, Thermo Scientific) and the other one with the BMH solvent DMSO. Both samples were rocked for 1 h at room temperature and then treated with 25 mM DTT for 15 min under continued rocking. The samples were spun in a bench top centrifuge for 5 min at maximal speed and concentrated by acetone precipitation. The resulting protein pellet was dissolved in 60  $\mu$ l 2X sample buffer with double the amount of  $\beta$ -mercaptoethanol. The samples were boiled for 5 min and probed for the proteins of interest by Western blot analysis.

### 3. Results

#### 3.1. The majority of HK1 in type II cells localizes to the mitochondria

The hydrophobic N-terminus of HK1 mediates a dynamic and regulated interaction with the mitochondria [20–22,28] (Fig. 1A). To verify those findings for the type II cervical carcinoma cell line HeLa, we immunostained endogenous HK1 in fixed cells and examined co-localization with a mitotracker dye in confocal fluorescence

microscopy (Fig. 1B). As expected, a large proportion of the HK1 signal overlapped with the mitochondrial staining, which suggests the presence of a mitochondrial HK1 population. However, a significant part of the HK1 signal did not co-localize with mitotracker, and presumably resided in the cytosol. To estimate the proportions of mitochondrial and cytosolic HK1, we performed cellular fractionation of type II HeLa and A549 lung carcinoma cells and tested the mitochondrial and cytosolic fractions for the presence of HK1. In both cell lines, the majority of HK1 co-fractionated with the mitochondria and only a minor fraction localized to the cytosol (Fig. 1C). We conclude that the majority of HK1 in type II cells localizes to the mitochondria.

#### 3.2. HK1 siRNA decreases the IMM potential

We then asked if depletion of HK1 has a pro-apoptotic phenotype at the mitochondria. One of the hallmarks of mitochondrial apoptotic signaling is the loss of mitochondrial membrane integrity, which causes

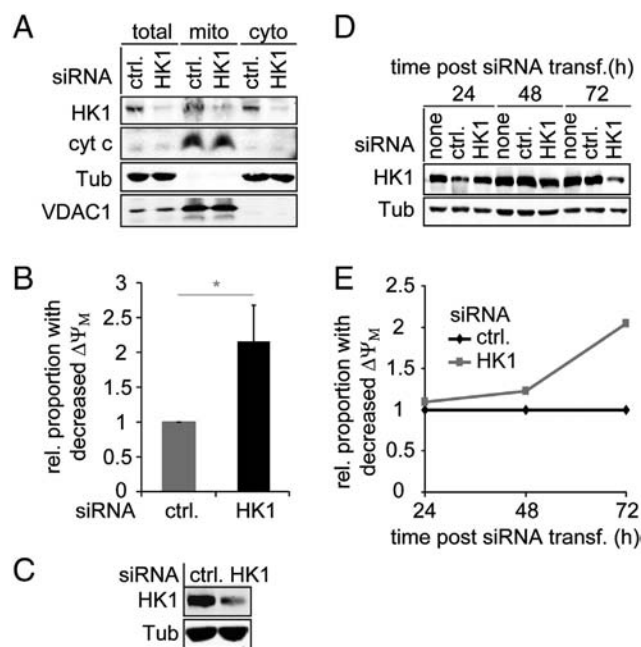


**Fig. 2.** HK1 siRNA decreases the IMM potential. A: Western blot of HK1 in total, heavy membrane/mitochondrial (mito) and cytosolic (cyto) fractions of HeLa cells treated with HK1 siRNA or a non-silencing control siRNA (ctrl.). All fractions were blotted for HK1, cytochrome c (cyt c), tubulin (Tub) and VDAC1. Tubulin and VDAC1 served as markers for cytosolic and mitochondrial fractions, respectively. B: Relative amount of cells with a reduced IMM potential ( $\Delta\Psi_M$ )/TMRE staining in a population of HeLa cells treated with HK1 siRNA or a non-silencing control siRNA (ctrl.). All values are presented as relative values to the proportion of control cells with reduced IMM potential, which was assigned a value of 1. 3 independent experiments were performed and presented as the mean + S.E.M. A significant difference ( $p < 0.05$ ) between the two experimental groups in the Student's T-test is indicated with \*. C: Western blot of HK1 expression in HeLa cells from panel B. Cells were treated with HK1 siRNA or non-silencing control siRNA (ctrl.). Total cell lysates were blotted for HK1 and tubulin (Tub) as a loading control. D: Western blot of the time course of siRNA-mediated HK1 depletion in HeLa cells. Cells were treated with the indicated siRNA duplexes and incubated for the indicated time periods and lysates were blotted for HK1 and tubulin (Tub) as a loading control. E: Representative time course of the relative amount of cells with reduced IMM potential ( $\Delta\Psi_M$ )/TMRE staining in HeLa cells from panel D. All values are relative to the proportion of control cells with reduced IMM potential at each individual time point, which was set to 1.

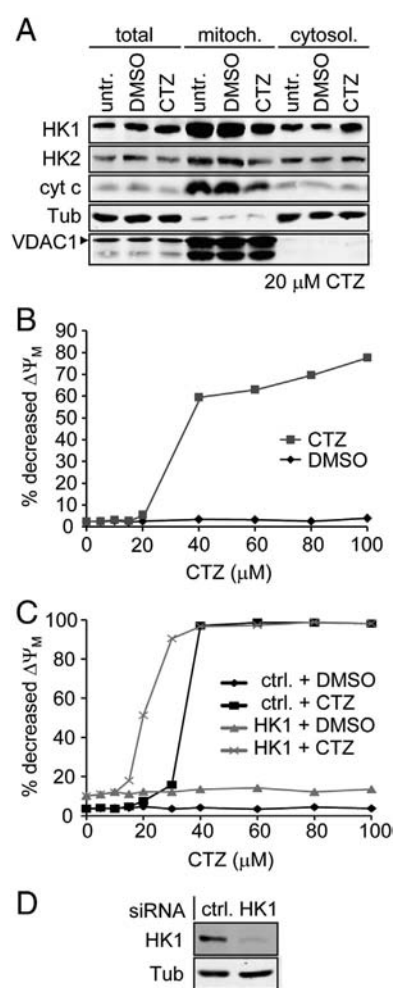


**Fig. 3.** CTZ decreases mitochondrial HKs, the IMM potential and mitochondrial integrity. A: Western blot of the total, heavy membrane/mitochondrial (mito), and cytosolic (cyto) fractions of HeLa cells treated with 20  $\mu$ M CTZ or DMSO for 1 h in serum-free medium (SFM). Fractions were probed with antibodies against HK1, HK2, cytochrome c (cyt c), tubulin (Tub), and VDAC1. Tubulin and VDAC1 served as markers for cytosolic and mitochondrial fractions, respectively. B: Representative graph of the percentage of cells with a reduced IMM potential ( $\Delta\Psi_M$ )/TMRE staining in a population of HeLa cells treated with the indicated concentrations of CTZ or DMSO for 1 h. C: Representative graph of the percentage of cells with a reduced IMM potential ( $\Delta\Psi_M$ )/TMRE staining in a population of HeLa cells pretreated with a control siRNA (ctrl.) or HK1 siRNA and treated with increasing concentrations of CTZ for 1 h. D: Western Blot of HK1 expression in HeLa cells from panel C. Lysates were probed with an antibody against HK1 and tubulin (Tub) as a loading control.

dissipation of the IMM potential [10,13]. The tetramethylrhodamine ethyl ester (TMRE) stain provides a convenient measure for the average IMM potential of cells. The cationic cell-permeable TMRE accumulates in the matrix of non-apoptotic, metabolically active mitochondria. We examined the IMM potential after siRNA-mediated depletion of HK1. Transfection of HeLa cells with HK1 siRNA and incubation for 3 days effectively depleted mitochondrial and cytosolic pools of HK1 in comparison to cells that were treated with a non-silencing control siRNA (Fig. 2A). We found that depletion of HK1 nearly doubled the number of cells with a decreased IMM potential compared to control cells (Fig. 2B,C). In a time course experiment, we noted that the decrease of HK1 protein levels on day 3 after siRNA transfection was paralleled by an increase of the population with a decreased IMM potential in a TMRE assay (Fig. 2D,E). We conclude that HK1 contributes to the integrity of mitochondrial membranes in type II cells.

### 3.3. CTZ displaces mitochondrial HKs and disrupts the IMM potential and mitochondrial integrity

To probe the link between mitochondrial HK1 and the IMM potential, we used a direct approach to detach HK1 from the mitochondria while keeping total cellular levels of HK1 constant. To this end, we used the anti-fungal imidazole derivative clotrimazole (CTZ), which diminishes the levels of mitochondrial HK activity [29] and protein [24,25]. A caveat for this study is that CTZ blocks the mitochondrial attachment of both HK1 and HK2 [24,25]. Accordingly, when we treated HeLa cells with CTZ, HK1 and HK2 levels decreased in the mitochondrial and increased in the cytosolic fraction (Fig. 3A). In contrast, treatment with the CTZ solvent DMSO did not affect the localization of HK1 or HK2. We then used the TMRE assay to monitor the effect of HK detachment from the mitochondria on the IMM potential. Treatment of HeLa cells with CTZ decreased the IMM potential in a concentration-dependent fashion. Low concentrations of CTZ did not affect the IMM potential, but CTZ concentrations of 20  $\mu$ M rapidly decreased IMM potential (Fig. 3B). Thus, the phenotype of CTZ treatment essentially

mirrors the phenotype of HK1 siRNA. Both treatments deplete the mitochondrial HK1 pool and decrease the IMM potential.

To test if the decrease of the IMM potential through CTZ was at least in part mediated by modification of mitochondrial HK1 levels and not just by a decrease of mitochondrial HK2 levels, we generated another CTZ concentration curve for cells that were pretreated with HK1 siRNA and compared it to cells treated with a non-silencing control siRNA (Fig. 3C,D). As expected, HK1 depletion decreased IMM potential. In addition, the threshold concentration for CTZ to decrease the IMM potential halved in HK1-depleted cells from 20  $\mu$ M to 10  $\mu$ M. These results demonstrate that depletion of HK1 facilitates the decrease of the IMM potential by CTZ and suggests that mitochondrial HK1 stabilizes the IMM potential. Loss of mitochondrial cytochrome c after detachment of mitochondrial HKs with CTZ (Fig. 3A) indicates that HKs maintain not only the IMM potential, but also mitochondrial membrane integrity.

### 3.4. CTZ accelerates TNF-induced apoptosis

We then asked if detachment of mitochondrial HKs with CTZ sensitizes cells to TNF-induced apoptosis. A combination of TNF and a sublethal dose of the translation inhibitor cycloheximide induces apoptosis with a concomitant dissipation of the IMM potential [18]. Addition of CTZ enhanced the loss of IMM potential (Fig. 4A). The number of cells with diminished IMM potential was more than twice as high in cells treated with TNF, cycloheximide and CTZ compared to cells treated with TNF, cycloheximide and DMSO. We obtained similar results when we monitored the apoptotic markers caspase-9 and PARP1 processing. Type II apoptotic signaling proceeds from the mitochondria to caspase-9, to effector caspases that cleave substrates such as PARP1 [7–9,15]. None of the individual treatments with TNF, cycloheximide, CTZ or DMSO led to the processing of caspase-9 or PARP1 (Fig. 4B). Combined treatment with TNF and cycloheximide resulted in a mild cleavage of caspase-9 and PARP1 by 8 h. When we administered TNF and cycloheximide in combination with CTZ, we observed a

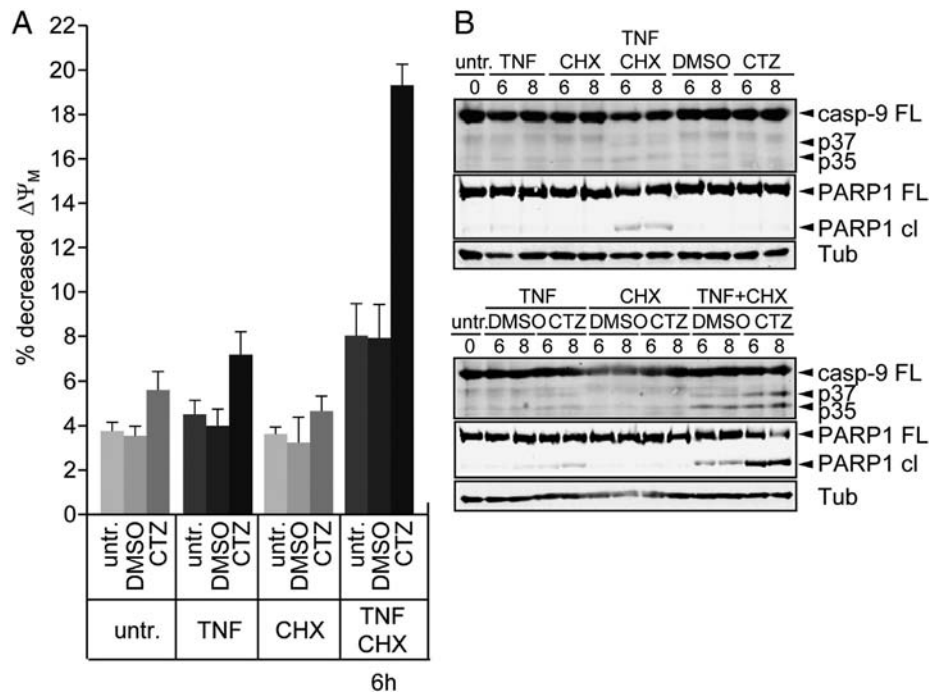


**Fig. 4.** CTZ accelerates TNF-induced apoptosis. A: Percentage of cells with reduced IMM potential ( $\Delta\Psi_M$ )/TMRE staining in a population of HeLa cells after treatment with the indicated combinations of TNF, cycloheximide (CHX), CTZ or DMSO for 6 hours. Values are presented as the mean + S.E.M. of 2 independent experiments. B: Western blot of caspase-9 and PARP1 cleavage in HeLa cells from panel A. Cell lysates for 0, 6, and 8 hour time points were probed with antibodies that detect full-length and p37 and p35 cleavage products of caspase-9 (casp-9), full-length (PARP1 FL) and p89 cleavage product (PARP1 cl) of PARP1, and tubulin (Tub) as a loading control.

pronounced increase of caspase-9 and PARP1 processing. We conclude that treatment with CTZ sensitizes cells to TNF-induced apoptosis.

### 3.5. Bcl-2 overexpression or Bak and Bax knockout stabilize the IMM potential after HK1 siRNA

Detachment of mitochondrial HKs through CTZ or HK2-specific peptides results in the accumulation of mitochondrial Bax and the release of mitochondrial stores of cytochrome c (Fig. 2A) [25,36,37]. These findings suggest that loss of mitochondrial HKs control the formation of Bax and possibly Bak-regulated channels in the OMM. We asked if overexpression of Bcl-2 attenuates the decrease of the IMM potential following HK1 depletion (Fig. 5A). Overexpression of Bcl-2 reverted the decreased IMM potential caused by HK1 depletion (Fig. 5B). In fact, there was no significant difference in the IMM potential of cells that overexpressed Bcl-2 after treatment with a non-silencing siRNA or a HK1 siRNA. We conclude that Bcl-2 overexpression inhibits the decrease of the IMM potential caused by loss of HK1.

As Bcl-2 controls the formation of Bak and Bax-regulated channels in the OMM [11], we asked if Bak and Bax channels in the OMM decrease the IMM potential after HK1 depletion. To address this question, we depleted HK1 from mouse embryonic fibroblast (MEF) cells with a deletion in the genomic bak and bax genes [30,31]. Wild type (wt) and Bak<sup>-/-</sup>/Bax<sup>-/-</sup> double knock-out (DKO) The cellular distribution of HK1 in MEFs was comparable to human type II cells (Fig. 5C, 1C).

MEFs expressed a relatively minor amount of HK2 that almost exclusively localized to the mitochondria (Fig. 5C).

Similar to our observations in human type II cells, loss of HK1 (Fig. 5D) significantly reduced the IMM potential of wt MEFs. In contrast, depletion of HK1 from cells deficient for Bax and Bax did not lead to a significant decrease of the IMM (Fig. 5E). These results show that HK1 stabilizes the IMM potential at least in part through the inhibition of Bak and/or Bax channels at the mitochondria.

### 3.6. HK1 depletion activates Bax

These findings prompted us to ask if HK1 controls the assembly of Bax channels on mitochondria. For these experiments, we pretreated HeLa cells with a control siRNA or a HK1 siRNA for 3 days and then incubated cells with a pro-apoptotic regime of TNF and cycloheximide. We then examined the co-fractionation of Bax and cytochrome c with mitochondrial and cytosolic fractions, respectively. Loss of HK1 clearly elevated mitochondrial Bax levels without an apoptotic stimulus. The amounts of mitochondrial Bax increased further in the presence of TNF and cycloheximide (Fig. 6A). Furthermore, loss of HK1 accelerated the accumulation of cytochrome c in the cytosol of cells treated with TNF and cycloheximide (Fig. 6A).

To examine the effect of HK1 depletion on the oligomerization of Bax, we incubated HeLa cells with a HK1 siRNA or a control siRNA and induced apoptosis with TNF and cycloheximide. We exposed lysates of the mitochondrial fraction to the cross-linker bismaleimido-hexane

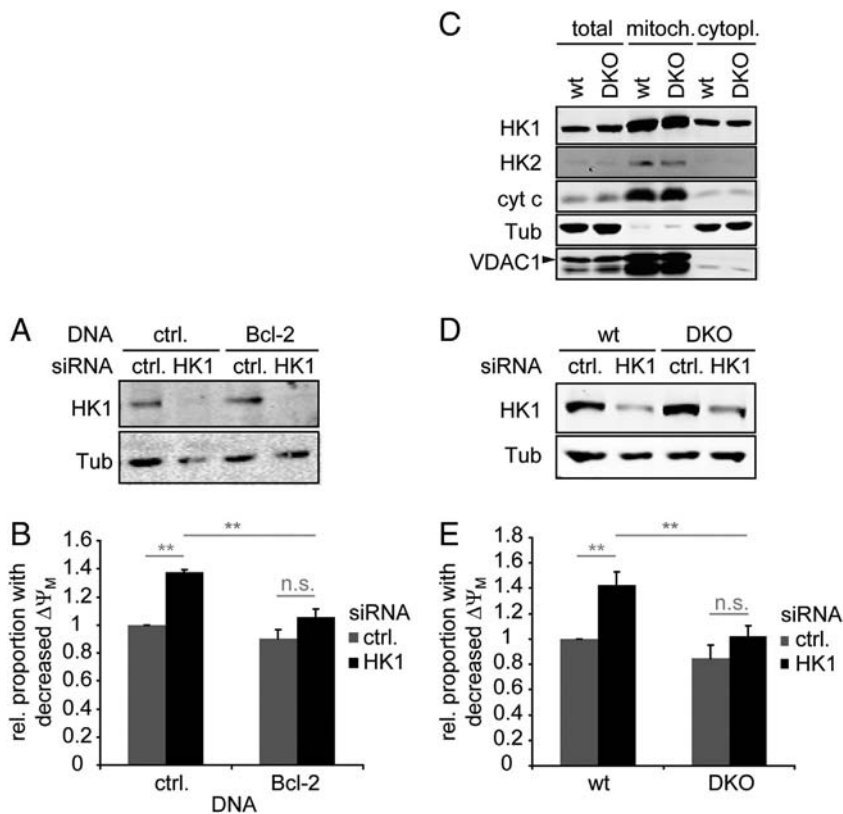


**Fig. 5.** Interactions between HK1 and Bcl-2 family members. **A:** Western blot of HK1 expression in HeLa cells transfected with HK1 siRNA or a non-silencing control siRNA (ctrl.) and a Bcl-2 expression construct or a control plasmid (ctrl.). Tubulin (Tub) served as a loading control. **B:** Relative proportion of HeLa cells with a reduced IMM potential ( $\Delta\Psi_M$ )/TMRE staining after transfection with HK1 siRNA or a non-silencing control siRNA (ctrl.) and a Bcl-2 expression construct or control plasmid (ctrl.). All values are reported relative to the proportion of cells with reduced IMM potential in the cell population transfected with control siRNA and plasmid and are presented as the mean  $\pm$  S.E.M. of 3 independent experiments. A significant difference between experimental groups in a Student's T-test with  $p < 0.01$  is indicated with \*\*, and a non-significant difference with n.s. **C:** Western blot of the total, heavy membrane/mitochondrial (mito), and cytosolic fractions of wild type (wt) and Bak<sup>-/-</sup>/Bax<sup>-/-</sup> double knock-out (DKO) MEFs. Fractions were probed for HK1, HK2, cytochrome c (cyt c), tubulin (Tub) and VDAC1. Tubulin and VDAC1 served as markers for cytosolic and mitochondrial fractions, respectively. **D:** Western Blot of HK1 expression in wild type (wt) and Bak<sup>-/-</sup>/Bax<sup>-/-</sup> double knock-out (DKO) MEF cells transfected with HK1 siRNA or a non-silencing control siRNA (ctrl.). Tubulin (Tub) served as a loading control. **E:** Relative proportion of cells with a reduced IMM potential ( $\Delta\Psi_M$ )/TMRE staining in wild type (wt) and Bak<sup>-/-</sup>/Bax<sup>-/-</sup> double knock-out (Bax/Bak DKO) MEFs after treatment with HK1 siRNA or a non-silencing control siRNA (ctrl.). All values are presented as the mean  $\pm$  S.E.M. of 4 independent experiments. A significant difference between experimental groups in the Student's T-test with  $p < 0.01$  is indicated with \*\*, and a non-significant difference with n.s.

(BMH) to covalently link Bax oligomers. In cells pre-incubated with a control siRNA, exposure to TNF and cycloheximide resulted in a gradual transition from monomeric Bax to dimeric, trimeric and tetrameric variants, consistent with the TNF-dependent formation of pro-apoptotic Bax channels in the OMM (Fig. 6B). In the absence of TNF and cycloheximide, the majority of mitochondrial Bax was monomeric in control cells (Fig. 6B). The amount of monomeric Bax decreased, and the amount of dimeric, trimeric and tetrameric Bax increased steadily upon treatment with TNF and cycloheximide. Loss of HK1 (Fig. 6C) accelerated the formation of higher state Bax oligomers in cells treated with HK1 siRNA in comparison to control cells. These data demonstrate that HK1 prevents mitochondrial membrane depolarization by controlling the formation of pro-apoptotic Bax channels in the OMM.

#### 4. Discussion

TNF triggers an array of reactions at sites of inflammation that includes secretion of pro-inflammatory cytokines, cell differentiation and proliferation, and the induction of cell death [1,2]. The beneficial effects of TNF and inflammation are often accompanied by undesirable effects such as tissue damage [2,32,33] or proliferative signals to tumors [34].

In this manuscript, we examined the mechanistic basis of HK1-mediated control of TNF-dependent apoptosis. HK1 is the most ubiquitously expressed of four human HK isoforms and like HK2, is highly expressed in cancers [19]. Both HKs have a hydrophobic N-terminus that allows interaction with mitochondria [21,22,35] and several studies implicated HK1 and HK2 in the control of cell survival [18,23,26,27,36]. Importantly, many of these studies detailed the relationship of mitochondrial hexokinases with pro-survival signals or intrinsic death signals. In contrast, relatively little is known about the molecular relationship of mitochondrial hexokinases and extrinsic apoptotic cues. Three previous studies displaced mitochondrial HK2 with a peptide with sequence identity to the N-terminus of HK2 [24,25,37]. The HK2 amino-terminal peptide released mitochondrial cytochrome c, decreased the IMM potential,

and induced nuclear fragmentation. In addition, it accelerated apoptosis induced by Bax-dependent indomethacin [25], or a combination of growth factor withdrawal and sublethal UV irradiation [24]. Given the similarities between HK1 and HK2, and the requirement for mitochondrial amplification of apoptotic signals in type II cells [7–9], we hypothesized that HK1 counters TNF-induced apoptosis at the mitochondria.

This hypothesis prompted us to explore the relationship between HK1 binding to the OMM, the IMM potential and apoptosis. The IMM potential dissipates when OMM and IMM integrity are compromised during apoptosis [10,13]. Bak and Bax channels in the OMM promote the loss of cytochrome c from the IMS and the influx of effector caspases during the later stages of apoptosis [10]. In later stages of apoptosis, the IMM may be permeabilized by MPTPs, which results in the complete collapse of the IMM potential [10,13]. CTZ treatment released mitochondrial cytochrome c and compromised OMM integrity. Release of cytochrome c requires reorganization of the mitochondria and includes remodeling of the IMM and opening of cristae junctions [10,13]. As depletion of HK1 decreased the IMM potential to a minor extent, we believe that loss of HK1 induced a decrease in OMM integrity that does not result in detectable release of cytochrome c. We showed that overexpression of the Bak and Bax antagonist Bcl-2 or absence of Bak and Bax blocked HK1 siRNA-mediated decrease of the IMM potential. These findings suggest that HK1 depletion allows the formation of Bak and Bax channels in the OMM. In line with that hypothesis we found that HK1 siRNA caused an increase in mitochondrial Bax, a weak increase in Bax oligomerization without TNF, and a pronounced acceleration of Bax oligomerization in cells that were incubated with TNF and cycloheximide.

A modification of Bax activation by mitochondrial HKs has been described elsewhere. For example, Pastorino et al. demonstrated that displacement of HK2 from mitochondria with CTZ or a specific HK2 peptide promoted mitochondrial localization of Bax, cytochrome c release and apoptosis [25]. Ectopic expression of HK2 had the opposite effect [25]. In other studies, expression of HK1 or the N-terminal hemidomain of HK2 attenuated exposure of the Bax N-terminus, while a decrease

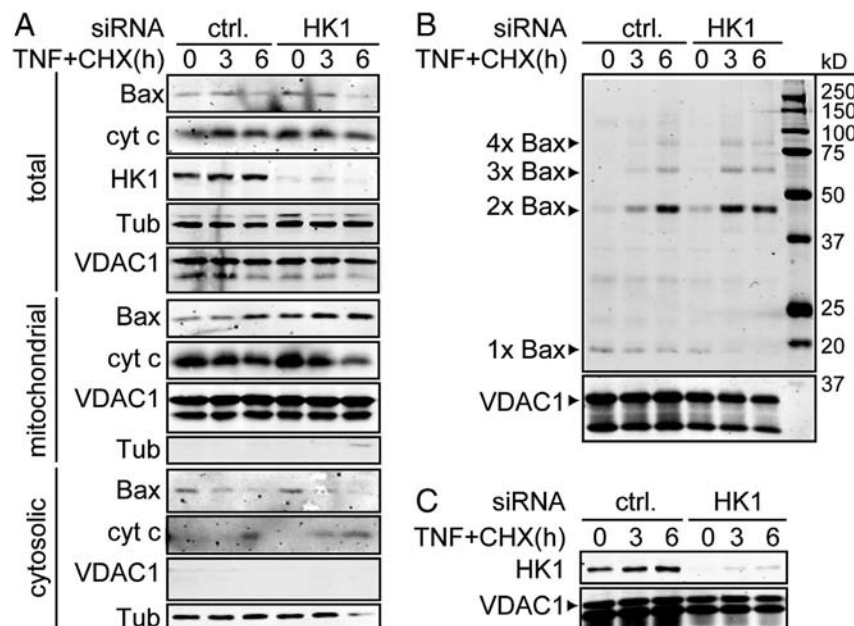


**Fig. 6.** HK1 depletion activates Bax. A: Western blot of the time course of Bax translocation to the mitochondria and release of cytochrome c from the mitochondria during TNF-induced apoptosis. HeLa cells were treated with HK1 siRNA or a non-silencing control siRNA (ctrl.) and incubated with TNF and cycloheximide (CHX) for the indicated time periods. Total, heavy membrane/mitochondrial and cytosolic fractions were probed for Bax, cytochrome c (cyt c), HK1, Tubulin (Tub) and VDAC1. Tubulin and VDAC1 served as markers for cytoplasmic and mitochondrial fractions, respectively. B: Western blot of Bax oligomerization in HeLa cells after pretreatment with HK1 siRNA or control siRNA (ctrl.) and treatment with TNF and cycloheximide for the indicated time periods. Lysates of the heavy membrane/mitochondrial fractions were incubated with the cross-linker BMH and probed with an antibody against Bax. Bax mono- and multimers are indicated. VDAC1 served as a loading control. C: Western blot of HK1 expression in the cell populations from B. VDAC1 served as a loading control.



of mitochondrial HK activity under glucose deprivation led to increased Bax oligomerization at the mitochondria [27,36]. We failed to detect a stable physical association of HK1 with Bak or Bax in co-precipitation studies. These observations lead us to propose that HK1 indirectly regulates the formation of pro-apoptotic mitochondrial pores by Bcl-2 family members, perhaps through antagonistic association with VDAC1.

In summary, we propose that mitochondrial HK1 antagonizes the activation and oligomerization of the Bcl-2 effector protein Bax and possibly Bak and stabilizes mitochondrial membrane integrity and IMM potential. Loss of mitochondrial HK1 through siRNA or CTZ activates Bax and possibly Bak, which decreases of OMM integrity and IMM potential. Engagement of death receptors in the absence of HK1 potentiates the activation of Bax and Bak and thereby accelerates the decrease of OMM integrity, the dissipation of the IMM potential, and the rate of pro-apoptotic caspase signaling.

## 5. Conclusions

HK1 is a mitochondrial protein that maintains the mitochondrial transmembrane potential of type II cells.

Displacement of mitochondrial hexokinases sensitizes cells to extrinsic apoptotic signals.

Anti-apoptotic Bcl-2 family members counter pro-apoptotic effects of HK1 and loss of HK1 accelerates the formation of Bak and Bax pores in mitochondria.

Our observations suggest that HK1 inhibits pro-apoptotic signals from TNF at mitochondria.

## Acknowledgements

HeLa cells were kindly provided by Dr. James Smiley, A549 cells by Dr. Michael Weinfeld, and wt MEF and Bak<sup>-/-</sup>, Bax<sup>-/-</sup> DKO MEF cells by Dr. Michele Barry (all University of Alberta, Edmonton, Alberta). The pcDNA3 vector (Invitrogen) and the pEGFP-N1 vector (Invitrogen) were received from Dr. Michele Barry, and the expression vector for human Bcl-2 from Dr. Ing Swie Goping (University of Alberta, Edmonton, Alberta). The research was funded by a grant from the Canadian Institutes of Health Research to EF (MOP 77746). EF holds a Canada Research Chair in Innate Immunity.

## References

- [1] E.R. Sherwood, T. Toliver-Kinsky, *Best Pract. Res. Clin. Anaesthesiol.* 18 (3) (2004) 385–405.
- [2] C. Nathan, *Nature* 420 (6917) (2002) 846–852.
- [3] H. Wajant, K. Pfizenmaier, P. Scheurich, *Cell Death Differ.* 10 (1) (2003) 45–65.
- [4] O. Micheau, J. Tschopp, *Cell* 114 (2) (2003) 181–190.
- [5] W. Schneider-Brachert, V. Tchikov, J. Neumeyer, M. Jakob, S. Winoto-Morbach, J. Held-Feindt, M. Heinrich, O. Merkel, M. Ehrenschrwender, D. Adam, et al., *Immunity* 21 (3) (2004) 415–428.
- [6] J. Dutta, Y. Fan, N. Gupta, G. Fan, C. Gelinas, *Oncogene* 25 (51) (2006) 6800–6816.
- [7] C. Scaffidi, S. Fulda, A. Srinivasan, C. Friesen, F. Li, K.J. Tomaselli, K.M. Debatin, P.H. Krammer, M.E. Peter, *EMBO J.* 17 (6) (1998) 1675–1687.
- [8] B.C. Barnhart, E.C. Alappat, M.E. Peter, *Semin. Immunol.* 15 (3) (2003) 185–193.
- [9] T. Kaufmann, A. Strasser, P.J. Jost, *Cell Death Differ.* 19 (1) (2012) 42–50.
- [10] S.W. Tait, D.R. Green, *Nat. Rev. Mol. Cell Biol.* 11 (9) (2010) 621–632.
- [11] J.E. Chipuk, T. Moldoveanu, F. Llambi, M.J. Parsons, D.R. Green, *Mol. Cell* 37 (3) (2010) 299–310.
- [12] L.D. Walensky, E. Gavathiotis, *Trends Biochem. Sci.* 36 (12) (2011) 642–652.
- [13] G. Kroemer, L. Galluzzi, C. Brenner, *Physiol. Rev.* 87 (1) (2007) 99–163.
- [14] S.J. Riedl, G.S. Salvesen, *Nat. Rev. Mol. Cell Biol.* 8 (5) (2007) 405–413.
- [15] R.C. Taylor, S.P. Cullen, S.J. Martin, *Nat. Rev. Mol. Cell Biol.* 9 (3) (2008) 231–241.
- [16] S.P. Cullen, S.J. Martin, *Cell Death Differ.* 16 (7) (2009) 935–938.
- [17] E.A. Slee, M.T. Harte, R.M. Kluck, B.B. Wolf, C.A. Casiano, D.D. Newmeyer, H.G. Wang, J.C. Reed, D.W. Nicholson, E.S. Alnemri, et al., *J. Cell Biol.* 144 (2) (1999) 281–292.
- [18] A. Schindler, E. Foley, *Cell. Signal.* 22 (9) (2010) 1330–1340.
- [19] J.E. Wilson, *J. Exp. Biol.* 206 (Pt 12) (2003) 2049–2057.
- [20] J.E. Wilson, *Trends Biochem. Sci.* 3 (1978) 124–125.
- [21] B.D. Gelb, V. Adams, S.N. Jones, L.D. Griffin, G.R. MacGregor, E.R. McCabe, *Proc. Natl. Acad. Sci. U. S. A.* 89 (1) (1992) 202–206.
- [22] P.G. Polakis, J.E. Wilson, *Arch. Biochem. Biophys.* 236 (1) (1985) 328–337.
- [23] K. Gottlob, N. Majewski, S. Kennedy, E. Kandel, R.B. Robey, N. Hay, *Genes Dev.* 15 (11) (2001) 1406–1418.
- [24] N. Majewski, V. Nogueira, P. Bhaskar, P.E. Coy, J.E. Skeen, K. Gottlob, N.S. Chandel, C.B. Thompson, R.B. Robey, N. Hay, *Molecular cell* 16 (5) (2004) 819–830.
- [25] J.G. Pastorino, N. Shulga, J.B. Hoek, *J. Biol. Chem.* 277 (9) (2002) 7610–7618.
- [26] J.M. Bryson, P.E. Coy, K. Gottlob, N. Hay, R.B. Robey, *J. Biol. Chem.* 277 (13) (2002) 11392–11400.
- [27] J.C. Rathmell, C.J. Fox, D.R. Plas, P.S. Hammerman, R.M. Cinali, C.B. Thompson, *Mol. Cell. Biol.* 23 (20) (2003) 7315–7328.
- [28] J.G. Pastorino, J.B. Hoek, *J. Bioenerg. Biomembr.* 40 (3) (2008) 171–182.
- [29] J. Penso, R. Beitner, *Eur. J. Pharmacol.* 342 (1) (1998) 113–117.
- [30] C.M. Knudson, K.S. Tung, W.G. Tourtellotte, G.A. Brown, S.J. Korsmeyer, *Science* 270 (5233) (1995) 96–99.
- [31] T. Lindsten, A.J. Ross, A. King, W.X. Zong, J.C. Rathmell, H.A. Shiels, E. Ulrich, K.G. Waymire, P. Mahar, K. Frauwirth, et al., *Molecular cell* 6 (6) (2000) 1389–1399.
- [32] C. Nathan, A. Ding, *Cell* 140 (6) (2010) 871–882.
- [33] R. Medzhitov, *Cell* 140 (6) (2010) 771–776.
- [34] S.I. Grivennikov, F.R. Greten, M. Karin, *Cell* 140 (6) (2010) 883–899.
- [35] M. Kurokawa, S. Oda, E. Tsubotani, H. Fujiwara, K. Yokoyama, S. Ishibashi, *Mol. Cell. Biochem.* 45 (3) (1982) 151–157.
- [36] N. Majewski, V. Nogueira, R.B. Robey, N. Hay, *Mol. Cell. Biol.* 24 (2) (2004) 730–740.
- [37] F. Chiara, D. Castellaro, O. Marin, V. Petronilli, W.S. Brusilow, M. Juhaszova, S.J. Sollott, M. Forte, P. Bernardi, A. Rasola, *PLoS One* 3 (3) (2008) e1852.